Squeezed lasing

Carlos Sánchez Muñoz (carlossmwolff@gmail.com)
Universidad Autónoma de Madrid https://orcid.org/0000-0001-8775-0135
Dieter Jaksch
University of Oxford https://orcid.org/0000-0002-9704-3941

Article

Keywords: squeezed laser, cavity mode, laser

Posted Date: September 11th, 2020

DOI: https://doi.org/10.21203/rs.3.rs-69491/v1

Squeezed lasing

Carlos Sánchez Muñoz[1,2] and Dieter Jaksch[1]

[1]*Clarendon Laboratory, University of Oxford, Parks Road, Oxford OX1 3PU, United Kingdom*
[2]*Departamento de Física Teórica de la Materia Condensada and Condensed Matter Physics Center (IFIMAC), Universidad Autónoma de Madrid, Madrid, Spain*[*]

(Dated: August 15, 2020)

We introduce the idea of a squeezed laser, in which a squeezed cavity mode develops a macroscopic photonic occupation powered by stimulated emission. Above the lasing threshold, the emitted light retains both the spectral purity inherent of a laser and the photon correlations characteristic of a photonic mode with squeezed quadratures. Our proposal, which can be implemented in optical setups, relies on the parametric driving of the cavity and dissipative stabilization by a broadband squeezed vacuum. We show that the squeezed laser can find applications going beyond those of standard lasers thanks to the squeezed character, such as enhanced operation in multi-photon microscopy or Heisenberg scaling of the Fisher information in quantum parameter estimation.

I. INTRODUCTION

The paradigm of a coherent squeezed state, consisting of a displaced squeezed vacuum, is routinely implemented in the laboratory by mixing laser light and squeezed vacua on a beam splitter. This approach has been used, for instance, to enhance the sensitivity of gravitational wave detectors beyond the shot-noise limit [1]. However, imperfect mode matching between the squeezed vacuum and the laser light limits the metrological applications of this method, and it represents one of the major challenges to overcome in order to reach the full potential for enhanced sensitivity provided by quadrature squeezing [2].

The origin of this problem lies in the fact that lasing and squeezing are taking place in different modes that need to be mixed a posteriori. The challenge posed by mode-matching could be overcome by a novel paradigm of lasing, in which the coherent squeezed state would be generated through the buildup of a macroscopic photon population by stimulated emission directly into a squeezed mode. This device, that we term here "squeezed laser", would yield a coherent squeezed state with the added characteristic features of a laser.

In this work, we propose an implementation of an optical squeezed laser and show that the squeezed lasing mechanism yields a coherent squeezed state retaining both the linewidth and coherence time characteristic of a laser, and the photon correlation properties of squeezed states. Our results can be understood from the perspective of the physics of driven-dissipative systems, where the extraordinary spectral purity of a laser emerges as the result of a second-order driven dissipative transition above which the Liouvillian gap is closed and coherence times diverge [3–5]. The squeezed laser opens the possibility to extend the range of applicability of narrowband non-classical states of light for bandwith-limited atom optics [6–9] and metrology [10–12], by capitalizing on the progress in the development of ultra-narrowband atom optics and lasers [3, 13, 14]. The quest for light-sources with narrow frequency spectra is motivated by applications such as quantum computing with trapped ions [15, 16], optical atomic clocks [17, 18], ground-state cooling of nanomechanical systems [19, 20], gravitational-wave detection [21, 22] geosciences [23] and tests of fundamental physics [24]. In this paper, we discuss potential applications of the squeezed laser for multi-photon microscopy and quantum parameter estimation.

Typically, squeezing is generated as a result of down-conversion in an optical parametric oscillator (OPO), in which a second-order dissipative phase transition also takes place [25]. Above the critical point, stimulated emission in the OPO yields a stationary state consisting of a mixture of macroscopic coherent states with opposing phases, and similarly to lasing, the Liouvillian gap closes, providing small narrow linewidth and long coherence times. However, squeezing in the OPO occurs below the phase transition. As one approaches the critical point from below, squeezing increases, but is also degraded by stimulated emission. Therefore, squeezing generation must occur below threshold and does not benefit from "lasing-like" properties, such as line-narrowing, that one can find well within the macroscopic phase above the transition point. Crucially, this is not the case in the mechanism of squeezed lasing that we propose here, in which squeezing takes place well within a macroscopic, lasing phase with the corresponding, divergent coherence times of a laser.

II. MODEL AND RESULTS

The mechanism that we propose requires driving the cavity that contains the gain medium by *i)* a detuned parametric drive, which modifies the nature of the photonic eigenstates, and *ii)* a resonant, broadband squeezed vacuum, which stabilizes the fluctuations (see Fig. 1).

Our model consists of a single cavity mode of frequency ω_c with bosonic annihilation operator a, interacting with N two-level atoms with ground and excited energy levels $\{|g\rangle_i, |e\rangle_i\}$, lowering operators $\sigma_i \equiv |g\rangle_i\langle e|_i$, and transition frequency ω_σ. The cavity is parametrically driven by a detuned drive of amplitude Ω_p, achieved through the down-conversion of a coherent drive of frequency $2\omega_p$ into photon pairs at frequency ω_p (slightly detuned from the cavity frequency ω_c)

* Corresponding author: carlossmwolff@gmail.com

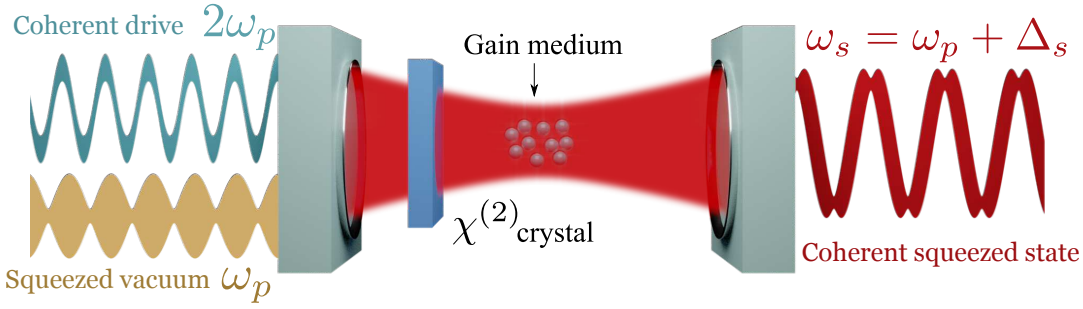

FIG. 1. Sketch of the proposed setup: a single cavity mode of frequency $\omega_c = \omega_p + \Delta_c$ (with $\Delta_c \ll \omega_p$) is parametrically driven through the down-conversion of pump photons of frequency $2\omega_p$ by a non-linear crystal $\chi^{(2)}$. The cavity includes a gain medium (e.g. an ensemble of two-level atoms) and is driven by a broadband squeezed vacuum centred at the frequency ω_p to stabilize lasing action. If the laser is imposed with a well-defined phase, the output emission corresponds to a coherent squeezed state of frequency $\omega_s = \omega_p + \Delta_s$.

by means of a non-linear $\chi^{(2)}$ crystal inside the cavity (see Fig. 1). A resonant version of this type of parametric drive is the typical mechanism to generate a squeezed vacuum just below the OPO threshold. Here, the coupling to the atoms will provide a gain mechanism, amplifying the vacuum of this squeezed mode into a coherent squeezed state by stimulated emission, and yielding laser-like coherence times. Contrary to the case of stimulated emission in the OPO phase transition, this macroscopic population buildup occurs into a squeezed mode and preserves the squeezing properties rather than degrading them. As we prove later, the pump intensities required to turn normal lasing action into lasing into a squeezed mode are well within reach in current experimental platforms.

In a frame rotating at a frequency ω_p, the total Hamiltonian reads ($\hbar = 1$)

$$H = \Delta_c a^\dagger a + \frac{\Omega_p}{2}(e^{i\theta}a^{\dagger 2} + \text{H.c}) + \sum_{i=1}^{N} \Delta_\sigma \sigma_i^\dagger \sigma_i + g(a^\dagger \sigma_i + a\sigma_i^\dagger), \tag{1}$$

with $\Delta_i \equiv \omega_i - \omega_p$, and θ the phase of the coherent drive. We have assumed a Jaynes-Cummings type of light-matter coupling, requiring the rotating-wave approximation (RWA) $g \ll \omega_c, \omega_\sigma$. The purely photonic part of the Hamiltonian can be diagonalized by a Bogoliouvov transformation corresponding to a unitary squeezing operator $S(re^{-i\theta}) = \exp\left[r(e^{i\theta}a^2 - e^{-i\theta}a^{\dagger 2})/2\right]$, with $r \equiv \ln[(1+\alpha)/(1-\alpha)]/4$, and $\alpha \equiv \Omega_p/\Delta_c$, so that $a \to a_s \cosh r - a_s^\dagger e^{-i\theta} \sinh r$, where a_s denotes the annihilation operator in the new, squeezed basis. The Hamiltonian then approximately becomes

$$H \approx \Delta_s a_s^\dagger a_s + \sum_{i=1}^{N} \Delta_\sigma \sigma_i^\dagger \sigma_i + \tilde{g}(a_s^\dagger \sigma_i + a_s \sigma_i^\dagger), \tag{2}$$

where $\Delta_s \equiv \Delta_c\sqrt{1-\alpha^2}$ and $\tilde{g} \equiv g\cosh r$. In the last step we have performed a new RWA under the requirement that the collective coupling remains small compared to the effective free frequencies, $\sqrt{N}g\sinh r \ll \Delta_s, \Delta_\sigma$. Although this requirement can in principle always be satisfied for any r by increasing both Δ_c and Ω_p so that the ratio α remains constant, it will ultimately be limited by the realistic impositions on the driving amplitude, Ω_p, and by the condition that Δ_c remains smaller than the free spectral range of the cavity, ω_{FSR}. The resulting light-matter coupling rate $\tilde{g}$ is exponentially enhanced with respect to the bare coupling by the factor $\cosh r$: this enhancement and its implications in different setups have been proposed and discussed in several works in recent years [26–29]. Here, we explore another consequence of this type of coupling: the possibility of developing a macroscopic photonic phase in the squeezed cavity mode a_s through a lasing mechanism.

To consider the possibility of squeezed lasing, we introduce a driven-dissipative model in which the previous Hamiltonian is supplemented by Lindblad operators that describe incoherent driving of the atoms and dissipative decay of cavity photons and atomic excitations. As has been discussed in previous works [26, 29], in order to avoid undesired noise when moving to the squeezed basis and achieve a decay that brings the system into the vacuum of the squeezed mode, an extra driving by a broadband squeezed vacuum is necessary. This can be achieved by driving the system with the output of an optical parametric oscillator of frequency ω_p and with a linewidth κ_s much larger than the cavity decay rate κ [30]. As we will see, the output will, in turn, provide coherent squeezed states with a linewidth that can be orders of magnitude smaller than κ.

As was discussed in [29], by tuning the squeezing parameter of the squeezed vacuum to $r_e = r$ and its phase to $\theta_e = \pi - \theta$, dissipation in the squeezed mode a_s turns into a normal decay term, and the resulting master equation for the atoms-cavity system reads

$$\dot{\rho} = -i[H,\rho] + \frac{\kappa}{2}D_{a_s}[\rho] + \sum_{i=1}^{N}\left[\frac{P}{2}D_{\sigma_i^\dagger}[\rho] + \frac{\gamma}{2}D_{\sigma_i}[\rho]\right], \tag{3}$$

where H is given by Eq. (2), and P and γ are, respectively, the incoherent pumping and spontaneous emission rates of the atoms.

The master equation (3) describes a basic model of a laser, which has been studied extensively [30]. Let us define the atom decay $\tilde{\gamma} \equiv (P+\gamma)/2$, the squeezed cooperativity $C_s =$

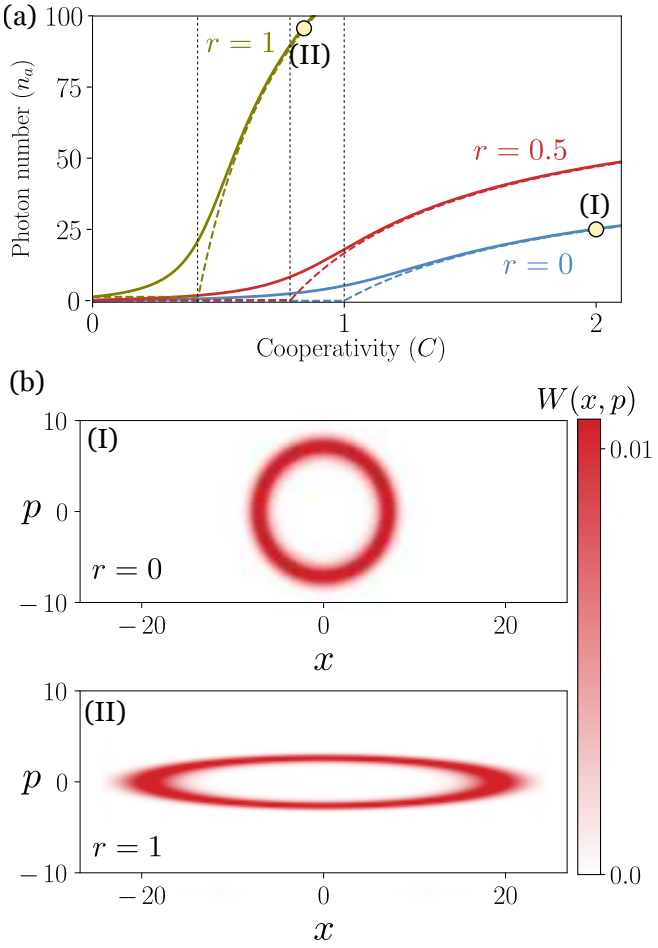

FIG. 2. (a) Lasing phase transition in terms of photon number versus cooperativity, for different values of the squeezing parameter r. Saturation photon number set as $n_q = 50$. Vertical lines mark the critical points, which are reduced for increasing r. Solid lines: exact numerical result. Dashed lines: mean field prediction. (b) Wigner function of the steady state corresponding to points (I) and (II) in panel (a), with $r = 0$ and 1 respectively, and $\theta = \pi$.

$2g_s^2/(\tilde{\gamma}\kappa)$, the pump parameter $p_s = NC_s(P-\gamma)/(P+\gamma)$ and the saturation parameter $n_0 = \tilde{\gamma}^2/2g_s^2$. A mean-field description of the Heisenberg equations of motion given by the ansatz $\langle a_s^\dagger \sigma\rangle = \langle a_s^\dagger\rangle\langle\sigma\rangle$ predicts a photon population $n_s \equiv \langle a_s^\dagger a_s\rangle$ featuring a dissipative phase transition at $p_s = 1$,

$$n_s = n_0(p_s - 1)H(p_s - 1), \tag{4}$$

were $H(x)$ denotes the Heaviside step function. Let us now consider this expression in terms of both the "bare" cooperativity $C = 2g^2/\kappa\tilde{\gamma}$ and pumping parameter $p = p_s C/C_s$. Given that $C_s = C\cosh^2 r$, the threshold condition $p_s = 1$ can be written as $p = 1/\cosh^2 r$. Therefore, one of the consequences of the parametric driving of the system is a reduction of the lasing pumping threshold by a factor $1/\cosh^2 r$.

Although many practical situations will require to consider a finite atomic decay $\gamma \neq 0$, for the sake of simplicity we will take the limit of a long-lived atomic transition $\gamma \to 0$, since the essential physics that we will discuss remains unchanged. By doing so the parameters above reduce to $p_s = NC_s$ and $n_0 = n_q/NC_s$, where $n_q = NP/2\kappa$ is the photon saturation number. The mean-field result thus predicts a phase transition at $p_s = 1$, with a photon population

$$n_s = n_q\left(1 - \frac{1}{p_s}\right)H(p_s - 1). \tag{5}$$

The photonic population in the bare cavity mode $n_a \equiv \langle a^\dagger a\rangle$ can be expressed in terms of n_s by undoing the squeezing transformation, which gives:

$$n_a = n_s\cosh(2r) + \sinh^2 r. \tag{6}$$

These results can be taken to the limit of the one-atom laser $N = 1$, where $p_s = C_s$. This limit is of practical and fundamental interest [31–36], particularly due to the thresholdless behaviour around the phase transition. From now on, we will consider this limit in all our calculations for the sake of convenience, since it will allow us to provide numerically exact results for the macroscopic cavity field. We will, however, be concerned with the deep-lasing regime, where the results are expected to be similar to the $N \gg 1$ case, converging to the mean-field prediction. There will be therefore no loss of generality.

Figure 2(a) depicts exact result for the stationary photon number n_a of the one-atom squeezed laser versus the cooperativity C for various values of r, together with the prediction of the mean-field ansatz. The exact solution depicts the well-known thresholdless behaviour of the one-atom laser [31], and it converges to the mean-field prediction at large values of the cooperativity. Despite the fact that the gain consists of a single atom, the system still features a notion of thermodynamic limit, which is reached when the photon saturation number, set by the ratio between P and κ, tends to infinity, $n_q \to \infty$. The photon number then approaches non-analytical behaviour of the mean-field prediction around the critical point.

Figure 2(b) shows the Wigner function of the lasing states corresponding to $r = 0$ and $r = 1$, at the points I and II marked in Fig. 2(a). These stationary states display a characteristic, non-gaussian annular shape due to phase diffusion. Well within the lasing phase, a lasing state is well approximated by a mixture of coherent states $|\sqrt{n_s}e^{i\varphi}\rangle$ with a fixed amplitude $\sqrt{n_s}$, mixed over all possible phases,

$$\rho_s = \frac{1}{2\pi}\int_0^{2\pi} d\varphi\, |\sqrt{n_s}e^{i\varphi}\rangle\langle\sqrt{n_s}e^{i\varphi}|. \tag{7}$$

In our system, this stationary state is developed in the squeezed basis. To recover the stationary photonic state of cavity mode in the original basis, ρ_a, we must apply a squeezing transformation, giving

$$\rho_a = \frac{1}{2\pi}\int_0^{2\pi} d\varphi\, S(re^{i\theta})|\sqrt{n_s}e^{i\varphi}\rangle\langle\sqrt{n_s}e^{i\varphi}|S(re^{i\theta})^\dagger. \tag{8}$$

This mixture of displaced-squeezed states gives the squeezed annular shape in phase space displayed at the bottom panel of

Fig. 2(b). To the best of our knowledge, a similar squeezed-lasing state has only been considered in a previous proposal in the microwave domain Ref. [36], which required a fast modulation of qubit energies in circuit quantum electrodynamics. Our proposal allows to implement this novel type of lasing in the optical domain, or any other system where a broadband squeezed vacuum and efficient down-conversion mechanisms are available.

III. EMISSION PROPERTIES

Having discussed the implementation, we now analyse the quantum-optical properties of the squeezed laser, with the aim of determining whether essential properties from both lasing and squeezing are unified in this light source. We therefore turn our attention to two fundamental characteristics that define both lasers and squeezed states: the spectral properties of the emission, and the fluctuation properties encoded in photonic correlations.

A. Spectrum of emission

Let us assume that the linewidth κ_s of the squeezed vacuum drive is $\kappa \ll \kappa_s \ll \Delta_s$, so that the input field at the emission frequency $\omega_p + \Delta_s$ can be considered to be vacuum. The spectrum of emission in the stationary limit $t \to \infty$ is then defined in terms of the Wiener-Khintchine formula [37]

$$S(\omega) = \lim_{t\to\infty} \frac{1}{\pi n_a} \mathrm{Re} \int_0^\infty d\tau\, e^{i\omega\tau} \langle a^\dagger(t) a(t+\tau)\rangle. \quad (9)$$

To relate the spectrum of the squeezed laser to that of a normal laser, it is convenient to rewrite the correlation function in terms of those of the squeezed mode. Writing $c \equiv \cosh r$, $s \equiv \sinh r$, we obtain:

$$\langle a^\dagger(t)a(t+\tau)\rangle = c^2\langle a_s^\dagger(t)a_s(t+\tau)\rangle + s^2\langle a_s(t)a_s^\dagger(t+\tau)\rangle + cs\left[e^{i\theta}\langle a_s^\dagger(t)a_s^\dagger(t+\tau)\rangle + e^{-i\theta}\langle a_s(t)a_s(t+\tau)\rangle\right]. \quad (10)$$

From the master equation (3), one can find that, in the stationary regime, any observable carrying phase information, such as $\langle a_s^2\rangle$, vanishes due to phase diffusion. This allows us to disregard the term proportional to cs in Eq. (10). Since the first two terms give similar contributions to the spectrum, we obtain $S(\omega) \propto S_s(\omega)$, where $S_s(\omega)$ is given by Eq. (9) with a substituted by a_s. Since the dynamics of the squeezed mode a_s, given by Eq. (3), is that of a standard laser, $S_s(\omega)$—and subsequently $S(\omega)$—corresponds to the spectrum of a laser with photon number n_s and cooperativity C_s. We can therefore conclude that the squeezed laser will inherit the spectral properties of a standard laser, including the extreme line narrowing developed in the lasing phase, with a linewidth that in the thermodynamic limit will be given by $\Gamma = \kappa C_s/4n_s$ [30]. The spectrum will be sharply peaked around the frequency of the squeezed mode $\omega_s \equiv \omega_p + \Delta_s$. Well within the lasing regime, this linewidth is inversely proportional to the saturation photon number n_q, and therefore will vanish in the thermodynamic limit $n_q \to \infty$. This trend is confirmed by numerical calculations of the spectrum of the squeezed laser, see Fig. 3, where we show the values of Γ extracted from the spectrum versus the effective cooperativity of the squeezed mode, C_s, and increasing values of the saturation photon number n_q.

Writing the lasing master equation Eq. (3) in terms of the Liouvillian superoperator, $\dot\rho = \mathcal{L}\rho$, the spectral linewidth Γ can equivalently be estimated from the Liouvillian gap, e.g., the eigenvalue λ_1 of the Liouvillian superoperator $\mathcal{L}$ with the second largest real part, so that $\Gamma \approx -2\,\mathrm{Re}\{\lambda_1\}$ (this relationship is discussed in more detail in [38]). Line-narrowing in lasing can therefore be understood as the result of a second-order driven-dissipative phase transition in which the Liouvillian gap is closed [3, 5]. Being so intertwined with the spectral properties of the Liouvillian, it is not surprising that the linewidth of the spectrum of emission is unchanged by a unitary transformation. As we will see, this is not the case for observables that quantify the correlation amongst the emitted photons.

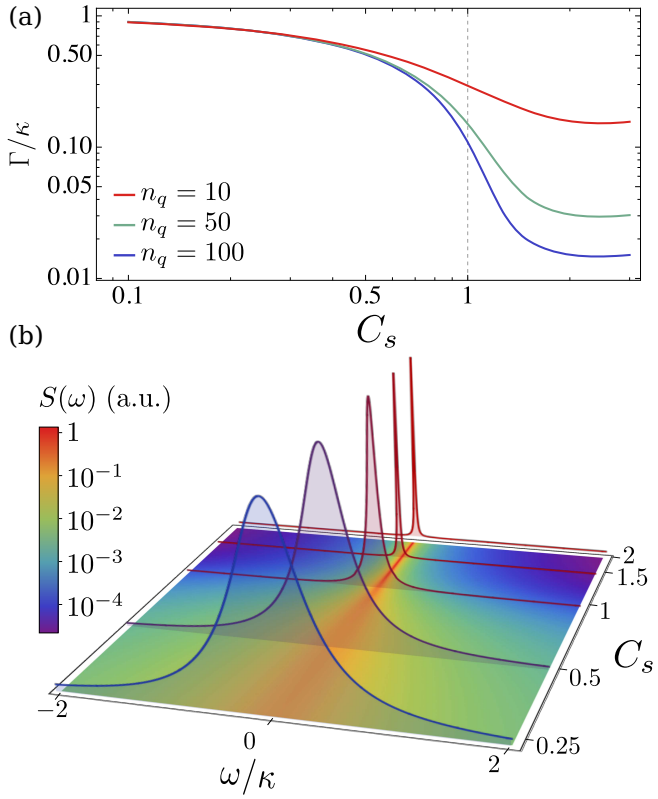

FIG. 3. Line narrowing of the emission spectrum in a squeezed laser. (a) Emission linewidth (related to phase diffusion rate) versus cooperativity C_s for different values of saturation photon number n_q. This result depends on r only through C_s. (b) Spectrum versus cooperativity C_s for saturation photon number $n_q = 100$. Frequency defined with respect to the squeezed mode frequency ω_s.

B. Quadrature squeezing

Most technological applications of squeezed states aim to exploit the reduced fluctuations in one of the quadratures of the field for metrological purposes [39–42]. It is therefore pertinent to ask whether the squeezed-lasing steady state given by Eq. (8) shows any degree of quadrature squeezing. Considering the quadratures $X_\phi = (ae^{-i\phi} + a^\dagger e^{i\phi})/2$, the squeezed quadrature with minimal fluctuations is the one with angle $\phi = \theta/2$. Fluctuations along these quadrature are given by

$$\langle \Delta X^2_{\theta/2} \rangle = e^{-2r}(2n_s + 1)/4. \tag{11}$$

As a consequence of the phase-diffusion, the exponential reduction of the quadrature fluctuations typical of a pure squeezed state is now multiplied by a factor $2n_s + 1$, which will yield squeezing, i.e. $\langle \Delta X^2_{\theta/2} \rangle < 1/4$, whenever $n_s < (e^{2r} - 1)/2$. While in the deep-lasing regime $n_s \gg 1$ this might likely not be the case, we have demonstrated in the previous section that the characteristic phase-diffusion timescale, given by $\tau_c = 1/\Gamma$, tends to diverge as the Liouvillian gap closes. Therefore, as it is usually done in the standard lasing scenario [43], it is meaningful to consider a transient, metastable symmetry-broken state, $\rho_\varphi = S(re^{i\theta})|\sqrt{n_s}e^{i\varphi}\rangle\langle\sqrt{n_s}e^{i\varphi}|S(re^{i\theta})^\dagger$ with a well-defined phase φ. This is simply a coherent squeezed state, as illustrated in Fig. 1. It is expected that this phase can be spontaneously picked by a system subjected to continuous, homodyne measurement [44] or seeded with a small, external field [4]. Notably, since the photon number distribution for this symmetry-broken state state depends on φ, we postulate that even a simple monitoring through photon-counting measurement could enforce the system to select a well-defined phase φ. We therefore assume that this phase can be imposed or post-selected, and that the corresponding symmetry-broken state ρ_φ is long-lived.

The amount of squeezing along a given quadrature X_ϕ for the state ρ_φ depends on both θ (fixed by the coherent drive) and φ. The quadrature $X_{\theta/2}$ remains the one with minimal fluctuations regardless the value of φ, and for an optimum phase $\varphi = (\theta \pm \pi)/2$, one recovers the degree of squeezing characteristic of a squeezed vacuum,

$$\langle \Delta X^2_{\theta/2} \rangle = e^{-2r}/4. \tag{12}$$

We can therefore assert that the squeezed laser can operate as a source of coherent squeezed states. Notably, even the phase-diffused state given by Eq. (8) features strong photon correlations with useful properties, as we describe below.

C. Second-order correlation function

A standard quantity to quantify correlations between photons is the second-order standard correlation function, defined in the stationary state as

$$g^{(2)}(\tau) = \lim_{t\to\infty} \frac{\langle a^\dagger(t)a^\dagger(t+\tau)a(t+\tau)a(t)\rangle}{\langle a^\dagger a(t)\rangle\langle a^\dagger a(t+\tau)\rangle}. \tag{13}$$

The introduction of this quantity and related ones by Glauber [45] in the context of the development of the first lasers established the notions of quantum-optical coherence and our theoretical understanding of ideal lasers as states that display coherence to all orders. Coherence to second-order would translate to $g^{(2)}(\tau) = 1$, as a consequence of photons in an ideal, standard laser being statistically independent.

The lasing system that we present here extends the definition of a laser in terms of Glauber's criterion of coherence. While the squeezed laser is a source of extremely monochromatic light with a characteristic coherence time $\tau_c = 1/\Gamma$ that tends to infinity in the thermodynamic limit, photons emitted by the squeezed laser exhibit positive correlations between each other, characterized by a value of the zero-delay, stationary second order correlation function $g^{(2)}(0)$ greater than one.

Considering the steady state given by Eq. (8), in the deep-lasing regime $n_s \gg 1$, $g^{(2)}(0)$ reads:

$$g^{(2)}(0) \approx \frac{3 - \mathrm{sech}(2r)^2}{2}, \tag{14}$$

which increases with the squeezing parameter r and saturates to a value $3/2$. For the symmetry-broken states ρ_φ considered above, this value can be made even larger. The good agreement with exact, numerical results is shown in Fig. 4(a).

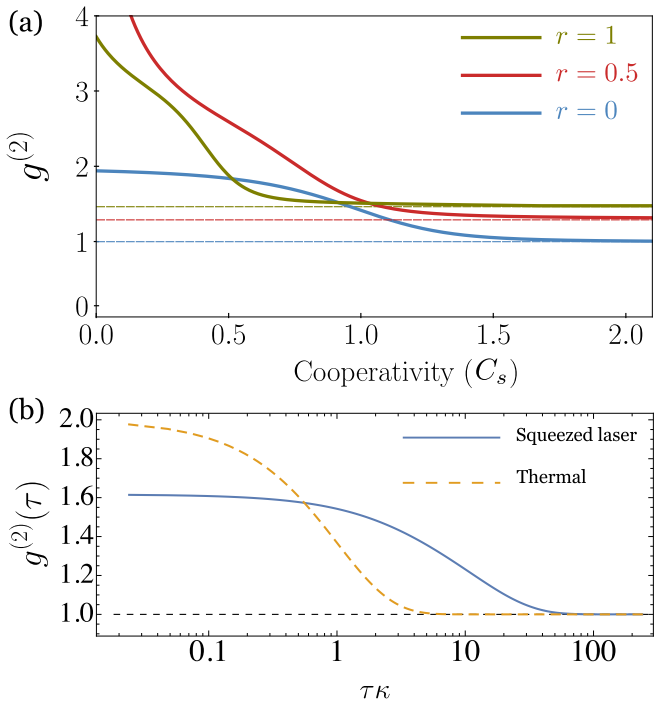

FIG. 4. Second-order correlation function. (a) Zero-delay second-order correlation function versus C_s for three values of squeezing parameter r and $n_q = 50$. Dashed lines correspond to the limit in the lasing regime given by Eq. (14). (b) $g^{(2)}(\tau)$ of the squeezed laser displaying positive correlations surviving for extremely long correlation times $\propto 1/\Gamma$. A thermal state, showed for comparison, displays a much shorter positive correlation time of the order $1/\kappa$. Parameters: $C_s = 1.5$, $r = 1$, $n_q = 50$.

Notably, and contrary to the case of e.g. a thermal state, these positive correlations exhibit an extraordinarily long coherence time τ_c, that can be made orders of magnitude longer than the natural lifetime of the cavity photons, $1/\kappa$, as shown in Fig . 4(b). These extremely long-lived positive correlations establish the squeezed laser as a novel source of light set apart from standard lasers or thermal sources. In the following, we explore some of the implications that these properties may have for prospective technological applications.

IV. TECHNOLOGICAL APPLICATIONS

After analysing the quantum optical characteristics of the squeezed laser, we now consider some of its properties related to its squeezed character that could be exploited for technological purposes. We discuss two of its potential applications: enhancement of multi-photon absorption and phase estimation in quantum metrology.

A. Multi-photon microscopy

The nonlinear process of multi-photon absorption, and in particular two-photon absorption (TPA), by an atomic or molecular system is the central element of key applications such as multi-photon microscopy or spectroscopy. Multi-photon microscopy has multiple advantages with respect to single-photon confocal microscopy [46–49]: for instance it provides enhanced spatial selectivity due to the quadratic scaling of multi-photon absorption rates with excitation intensity, which makes TPA only possible at the focal plane, and also allows for deeper penetration lengths in biological samples due to the longer wavelength of the illuminating field. The use of non-classical light with entangled or strongly-correlated photons have been proposed theoretically [50, 51] and confirmed experimentally [52–55] in order to strongly increase the TPA probability and reduced the require intensity of the illuminating field.

A simple expression of the TPA rate w_2 based on perturbation theory was derived by Mollow [56] in the late 60's: it depends on the linewidth κ_f of the final state and the second-order correlation function of the illuminating field, and notably, if the bandwith of this field is small compared to the width of the final state $\Delta\omega \ll \kappa_f$, w_2 at the two-photon resonance reduces to:

$$w_2 = \frac{4|g|^2}{\kappa_f} G^{(2)}(0), \tag{15}$$

where g is the light-matter coupling rate and $G^{(2)}(0) = \langle {a^\dagger}^2 a^2 \rangle$. The extremely narrow bandwith of the squeezed laser allows us to work under this assumption. Since for a classical, coherent field $G^{(2)}(0) \propto n_a^2$, the factor of improvement of the two-photon rate with respect to a classical field with the same intensity is given by the normalized, second-order correlation function $f = w_2/w_{2,\text{class}} = G^{(2)}(0)/n_a^2 = g^{(2)}(0)$. Therefore, the positive correlations $g^{(2)}(0) > 1$ in the squeezed laser makes it a possible candidate for TPA microscopy and spectroscopy with laser light featuring an increased two-photon absorption rate with respect to a standard laser.

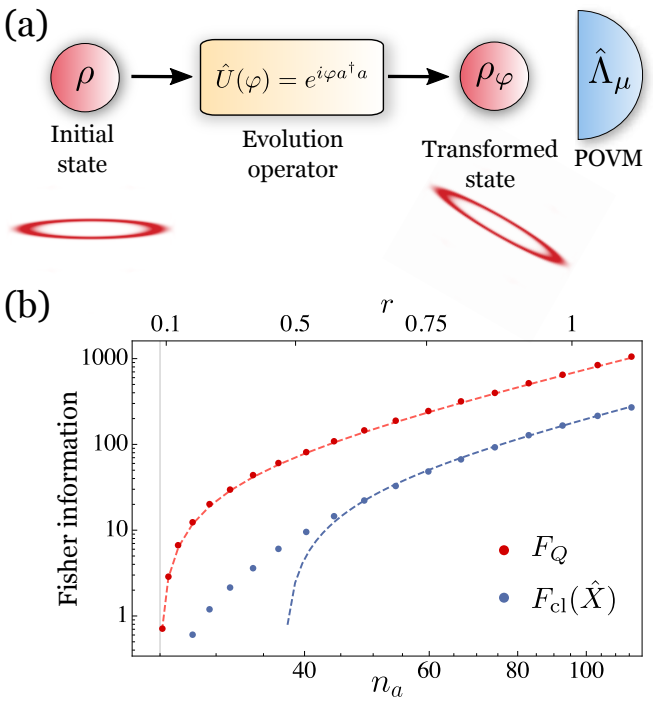

FIG. 5. (a) Quantum parameter estimation. (b) Fisher information versus average photon number.

B. Quantum Parameter Estimation

To discuss the possible metrological applications of the squeezed laser, we consider the paradigm of quantum parameter estimation shown in Fig. 5(a). The aim is to measure a phase φ which has been encoded in a state ρ_φ. This encoding takes place through a unitary transformation $\hat{U}_\varphi$, dependent on φ, applied onto an initially prepared state ρ_0. In our case, the initial state is the steady state of the squeezed laser, Eq. (8), and we consider a transformation given by simple phase rotation, $\hat{U}_\varphi = \exp\left[i\varphi a^\dagger a\right]$.

We then perform a generalized quantum measurement given by a positive operator-valued measure (POVM). A POVM consist of a series of operators Λ_μ, with $\mu \in \{1, 2, \dots M\}$ denoting the outcome of the measurement, whose probability of occurring is $p_\varphi(\mu) = \text{Tr}[\rho_\varphi \Lambda_\mu]$. To ensure that $p\varphi(\mu)$ is a valid probability distribution, the elements of the POVM must add up to the identity, $\sum_\mu \Lambda_\mu = \mathbb{1}$. Our goal is to estimate φ from the outcome of the measurements.

For ν measurement outcomes, the classical Cramer-Crao bound establishes that the minimal mean-square error in our estimation of φ is given by $\Delta^2\varphi \geq 1/\nu F(p_\varphi)$, where $F(p_\varphi) = E\left[-\frac{\mathrm{d}^2}{\mathrm{d}\varphi^2} \log p_\varphi\right]$ is the Fisher information of the

probability distribution [39, 41, 57]. An upper bound of the Fisher information that is independent of the POVM and that relies only on the state encoding ρ_φ is the quantum Fisher information F_Q, defined as optimum Fisher information over all possible POVMs, $F_Q(\rho_\varphi) = \max_{\Lambda_\mu} F(\rho_\varphi, \Lambda_\mu)$. In the case in which the estimated parameter is encoded in the state via a unitary transformation $U_\varphi = \exp[-iH\varphi]$, the quantum Fisher information can be computed as

$$F_Q = \sum_{i,j} \frac{2|\langle e_i|H|e_j\rangle|^2(\lambda_i - \lambda_j)^2}{\lambda_i + \lambda_j} \tag{16}$$

where $|e_i\rangle$ and λ_i are the eigenvalues and eigenvectors of the initial state ρ_0 [39]. In this case, the quantum Fisher information is independent of φ. If the estimated parameter is encoded in a photonic state ρ_φ with mean photon number n_a, the limit for the scaling of the precision of our estimation is set by the shot-noise limit $\Delta\varphi \propto 1/\sqrt{n_a}$ for a classical state. However, quantum, entangled states can surpass this limit and reach a scaling $\Delta\varphi \propto 1/n_a$, known as the Heisenberg limit [41].

A key metrological feature of squeezed vacuum is that it can provide Heisenberg scaling of the Fisher information when mixed with a coherent state in the input of a Mach-Zender interferometer [58]. Here, we show that the squeezed laser can similarly achieve Heisenberg scaling on the even simpler configuration displayed in Fig. 5(a), e.g. without the need of signal mixing in an interferometer. To prove this, we compute the quantum Fisher information using Eq. (16) and setting ρ_0 as ρ_a in Eq. (8). This state is completely determined by two variables: the photonic population in the squeezed mode n_s and the squeezing parameter r. The photonic population in the bare cavity mode is given by Eq. (6), and can be increased by increasing both n_s and r. As we show in Fig. 5(b), we can achieve Heisenberg scaling if the photonic population n_a (given by Eq. (6)) is increased by setting n_s constant and increasing r. We have numerically confirmed that, in that case, the quantum Fisher information is well approximated by

$$F_Q \approx \frac{1}{n_s}(n_a^2 - n_s^2), \tag{17}$$

displaying Heisenberg scaling $F_Q \propto n_a^2$. In a similar configuration, we have also verified that the classical Fisher information associated to the measurement of $\hat{X} = a + a^\dagger$ displays Heisenberg scaling for sufficiently large n_a. Our results further confirm that the squeezed laser inherits not only the properties of linewidth narrowing of a standard laser, but also the metrological properties of squeezed states. Notably, and contrary to standard approaches, this does not require the mixing of two modes (coherent and squeezed) in a beamsplitter, since this mixed character is an inherent property of the squeezed laser. This can allow to overcome difficulties associated to mode mixing, such as losses or the need of exact mode-matching.

V. EXPERIMENTAL IMPLEMENTATION

There are two main constraints for the experimental implementation of the squeezed laser. The first one is imposed by the requirement for a squeezed vacuum with a bandwith much larger than the cavity linewidth, so that it behaves effectively as a squeezed white noise. The second one is the condition $\sqrt{N}g\sinh r \ll \Delta_s$, which is required to apply a rotating-wave approximation and obtain a Jaynes-Cummings type of coupling between the atoms and the squeezed cavity mode. Therefore, if one desires to achieve a specific value of r (determined by the ratio Ω_p/Δ_c), one needs to increase Δ_c and Ω_p by the same factor until the condition is fulfilled, which might be ultimately limited by the maximum possible power available for the pump and by the free spectral range of the cavity, which should remain larger than the required detuning.

To address these questions, we will take as a reference example recent experiments on superradiant lasing in cold strontium [13, 59]. Here, lasing occurs in a long-lived ($\gamma = 7.5\,\mathrm{kHz}$) dipole-forbidden $^3\mathrm{P}_1 \rightarrow {}^1\mathrm{S}_0$ transition in ^{88}Sr, corresponding to a frequency $\omega_c/2\pi = 435\,\mathrm{THz}$ and with an effective, collective light-matter coupling between atoms and cavity mode $\sqrt{N}g/2\pi \sim 1\,\mathrm{MHz}$ [13]. We consider cavities with a linewidth going from $\kappa/2\pi = 160\,\mathrm{kHz}$ as reported in Ref. [13], to the more typical values of $\kappa/2\pi \sim 2\,\mathrm{MHz}$ common in cavity-QED experiments [60].

The requirement of squeezed noise with a broad enough bandwith can be met with several, broadband squeezed vacua with bandwidths much larger than MHz that have been reported experimentally, with examples ranging from 65 MHz in ring optical parametric oscillators [61] to 1.2 GHz in monolithic PPKTP cavities [62].

Regarding the RWA condition, consider that we require a squeezed laser with a value of $r = 1$, which in the case of a squeezed vacuum corresponds to a reduction of quadrature variance of $\sim 8.5\,\mathrm{dB}$. This value of r is obtained by setting $\alpha \approx 0.46$. The RWA will only hold if $\Delta_c\sqrt{1-\alpha^2} \approx 0.88\Delta_c \gg \sqrt{N}g\sinh(1)$, which is fulfilled for $\Delta_c \gg \sqrt{N}g$. Assuming $\Delta_c/2\pi = 20 \times g/2\pi \sim 20\,\mathrm{MHz}$, we would require $\Omega_p \sim 10\,\mathrm{MHz}$. In a doubly-resonant situation in which the cavity is resonant with both pumping and signal fields, Ω_p is related to the power P of the pump by $P = A_p(\Omega_p/\kappa)^2 P_0$ [63], where A_p is the waist area of the pump beam, and P_0 is given by

$$P_0 = \frac{\epsilon_0 c^3 n_0^2 T_p T_s^2}{32(\chi l \omega_c)^2}, \tag{18}$$

with n_0, l and χ the index of refraction, length and nonlinear susceptibility of the nonlinear crystal, ω_c the frequency of the cavity mode, and $T_{s(p)}$ the cavity transmission factor at the signal (pump) frequencies. Using typical parameters for a PPKTP crystal, $l = 0.5\,\mathrm{mm}$, $\chi = 14\,\mathrm{pm/V}$ and $n_0 = 1.8$ [40], and taking $T_p = T_s = T \approx 1.3 \times 10^{-4}$ consistent with a free spectral range $\omega_{\mathrm{FSR}}/2\pi \approx 2.6\,\mathrm{GHz}$ and $\kappa/2\pi = 160\,\mathrm{kHz}$ [13], and a waist radius of the pump beam of $30\,\mu\mathrm{m}$, the resulting required power would be $P \sim 1.5\,\mu\mathrm{W}$. In a worse scenario in which the cavity had transmissivity

$T \sim 10^{-2}$ and $\kappa/2\pi \approx 2\,\mathrm{MHz}$ ($\omega_{\mathrm{FSR}}/2\pi \approx 400\,\mathrm{MHz}$), the required power would raise $P \approx 4.6\,\mathrm{mW}$. We see that in any of these situations, the required pumping power would remain within reasonable values not above the order of mW, and the free spectral range of the cavity would remain smaller than the required detuning $\Delta_c \sim 20\,\mathrm{MHz}$.

VI. CONCLUSIONS

We have introduced the concept of a squeezed laser that can be implemented in optical setups. In contrast to the standard definition in terms of Glauber's criterion of coherence, the squeezed laser features photon correlations $g^{(2)}(0) > 1$ due to the squeezed character, together with extremely narrow linewidth and long coherence times typical of a laser. We have shown that this novel source of light might prove relevant in technological applications where the spectral purity of a laser is required, but photonic correlations typical of squeezed states are beneficial, such as multi-photon microscopy or quantum parameter estimation.

ACKNOWLEDGMENTS

C.S.M. thanks C. Navarrete-Benlloch for insightful discussions and advice. Both authors acknowledge funding from the European Research Council under the European Union's Seventh Framework Programme (FP7/2007-2013)/ERC Grant Agreement No. 319286 (Q-MAC). C.S.M. has been supported by the Marie Sklodowska-Curie Fellowship QUSON (Project No. 752180). DJ acknowledges funding from the EPSRC Hub in Quantum Computing and Simulation (EP/T001062/1).

[1] J. Aasi, J. Abadie, B. P. Abbott, R. Abbott, T. D. Abbott, M. R. Abernathy, C. Adams, T. Adams, P. Addesso, R. X. Adhikari, *et al.*, Enhanced sensitivity of the LIGO gravitational wave detector by using squeezed states of light, Nature Photonics **7**, 613 (2013).

[2] E. Oelker, L. Barsotti, S. Dwyer, D. Sigg, and N. Mavalvala, Squeezed light for advanced gravitational wave detectors and beyond, Optics Express **22**, 21106 (2014).

[3] E. M. Kessler, G. Giedke, A. Imamoglu, S. F. Yelin, M. D. Lukin, and J. I. Cirac, Dissipative phase transition in a central spin system, Physical Review A **86**, 012116 (2012).

[4] S. Fernández-Lorenzo and D. Porras, Quantum sensing close to a dissipative phase transition: Symmetry breaking and criticality as metrological resources, Physical Review A **96**, 1 (2017).

[5] F. Minganti, A. Biella, N. Bartolo, and C. Ciuti, Spectral theory of Liouvillians for dissipative phase transitions, Physical Review A **98**, 42118 (2018).

[6] T. Tanimura, D. Akamatsu, Y. Yokoi, A. Furusawa, and M. Kozuma, Generation of a squeezed vacuum resonant on a rubidium D1 line with periodically poled KTiOPO4, Optics Letters **31**, 2344 (2006).

[7] G. Hétet, O. Glöckl, K. A. Pilypas, C. C. Harb, B. C. Buchler, H. A. Bachor, and P. K. Lam, Squeezed light for bandwidth-limited atom optics experiments at the rubidium D1 line, Journal of Physics B: Atomic, Molecular and Optical Physics **40**, 221 (2007).

[8] J. Appel, E. Figueroa, D. Korystov, M. Lobino, and A. I. Lvovsky, Quantum Memory for Squeezed Light, Physical Review Letters **100**, 093602 (2008).

[9] K. Honda, D. Akamatsu, M. Arikawa, Y. Yokoi, K. Akiba, S. Nagatsuka, T. Tanimura, A. Furusawa, and M. Kozuma, Storage and Retrieval of a Squeezed Vacuum, Physical Review Letters **100**, 093601 (2008).

[10] F. Wolfgramm, A. Cerè, F. A. Beduini, A. Predojević, M. Koschorreck, and M. W. Mitchell, Squeezed-Light Optical Magnetometry, Physical Review Letters **105**, 053601 (2010).

[11] F. Wolfgramm, C. Vitelli, F. A. Beduini, N. Godbout, and M. W. Mitchell, Entanglement-enhanced probing of a delicate material system, Nature Photonics **7**, 28 (2013).

[12] T. Horrom, R. Singh, J. P. Dowling, and E. E. Mikhailov, Quantum-enhanced magnetometer with low-frequency squeezing, Physical Review A **86**, 023803 (2012).

[13] M. A. Norcia and J. K. Thompson, Cold-Strontium Laser in the Superradiant Crossover Regime, Physical Review X **6**, 011025 (2016).

[14] M. N. Winchester, M. A. Norcia, J. R. Cline, and J. K. Thompson, Magnetically Induced Optical Transparency on a Forbidden Transition in Strontium for Cavity-Enhanced Spectroscopy, Physical Review Letters **118**, 263601 (2017).

[15] D. Leibfried, R. Blatt, C. Monroe, and D. Wineland, Quantum dynamics of single trapped ions, Reviews of Modern Physics **75**, 281 (2003).

[16] H. Häffner, C. F. Roos, and R. Blatt, Quantum computing with trapped ions, Physics Reports **469**, 155 (2008).

[17] A. D. Ludlow, M. M. Boyd, J. Ye, E. Peik, and P. O. Schmidt, Optical atomic clocks, Reviews of Modern Physics **87**, 637 (2015).

[18] I. Ushijima, M. Takamoto, M. Das, T. Ohkubo, and H. Katori, Cryogenic optical lattice clocks, Nature Photonics **9**, 185 (2015).

[19] J. D. Teufel, T. Donner, D. Li, J. W. Harlow, M. S. Allman, K. Cicak, A. J. Sirois, J. D. Whittaker, K. W. Lehnert, and R. W. Simmonds, Sideband cooling of micromechanical motion to the quantum ground state, Nature **475**, 359 (2011).

[20] U. Delić, M. Reisenbauer, K. Dare, D. Grass, V. Vuletić, N. Kiesel, and M. Aspelmeyer, Cooling of a levitated nanoparticle to the motional quantum ground state, Science **367**, 892 (2020).

[21] G. Cagnoli, L. Gammaitoni, J. Hough, J. Kovalik, S. McIntosh, M. Punturo, and S. Rowan, Very High Q Measurements on a Fused Silica Monolithic Pendulum for Use in Enhanced Gravity Wave Detectors, Physical Review Letters **85**, 2442 (2000).

[22] F. Acernese, M. Alshourbagy, F. Antonucci, S. Aoudia, K. G. Arun, P. Astone, G. Ballardin, F. Barone, L. Barsotti, Barsuglia, *et al.*, Laser with an in-loop relative frequency stability of 1.0× 10-21 on a 100-ms time scale for gravitational-wave detection, Physical Review A **79**, 053824 (2009).

[23] T. Takano, M. Takamoto, I. Ushijima, N. Ohmae, T. Akatsuka, A. Yamaguchi, Y. Kuroishi, H. Munekane, B. Miyahara,

and H. Katori, Geopotential measurements with synchronously linked optical lattice clocks, Nature Photonics **10**, 662 (2016).
[24] M. S. Safronova, D. Budker, D. Demille, D. F. Kimball, A. Derevianko, and C. W. Clark, Search for new physics with atoms and molecules, Reviews of Modern Physics **90**, 25008 (2018).
[25] D. F. Walls and G. J. Milburn, *Quantum Optics* (Springer-Verlag, 1994).
[26] M. A. Lemonde, N. Didier, and A. A. Clerk, Enhanced nonlinear interactions in quantum optomechanics via mechanical amplification, Nature Communications **7**, 1 (2016).
[27] S. Zeytinoglu, A. Imamoglu, and S. Huber, Engineering matter interactions using squeezed vacuum, Physical Review X **7**, 021041 (2017).
[28] C. Leroux, L. C. Govia, and A. A. Clerk, Enhancing Cavity Quantum Electrodynamics via Antisqueezing: Synthetic Ultrastrong Coupling, Physical Review Letters **120**, 93602 (2018).
[29] W. Qin, A. Miranowicz, P. B. Li, X. Y. Lü, J. Q. You, and F. Nori, Exponentially Enhanced Light-Matter Interaction, Cooperativities, and Steady-State Entanglement Using Parametric Amplification, Physical Review Letters **120**, 93601 (2018).
[30] G. W. Gardiner and P. Zoller, *Quantum Noise*, 2nd ed. (Springer-Verlag, Berlin, 2000).
[31] J. McKeever, A. Boca, A. D. Boozer, J. R. Buck, and H. J. Kimble, Experimental realization of a one-atom laser in the regime of strong coupling, Nature **425**, 268 (2003).
[32] A. D. Boozer, A. Boca, J. R. Buck, J. McKeever, and H. J. Kimble, Comparison of theory and experiment for a one-atom laser in a regime of strong coupling, Physical Review A **70**, 023814 (2004).
[33] L. Florescu, S. John, T. Quang, and R. Wang, Theory of a one-atom laser in a photonic band-gap microchip, Physical Review A **69**, 013816 (2004).
[34] O. Astafiev, K. Inomata, A. O. Niskanen, T. Yamamoto, Y. A. Pashkin, Y. Nakamura, and J. S. Tsai, Single artificial-atom lasing, Nature **449**, 588 (2007).
[35] F. Dubin, C. Russo, H. G. Barros, A. Stute, C. Becher, P. O. Schmidt, and R. Blatt, Quantum to classical transition in a single-ion laser, Nature Physics **6**, 350 (2010).
[36] C. Navarrete-Benlloch, J. J. García-Ripoll, and D. Porras, Inducing nonclassical lasing via periodic drivings in circuit quantum electrodynamics, Physical Review Letters **113**, 193601 (2014).
[37] J. H. Eberly, Atomic relaxation in the presence of intense partially coherent radiation fields, Phys. Rev. Lett. **37** (1976).
[38] C. Sánchez Muñoz, B. Buča, J. Tindall, A. González-Tudela, D. Jaksch, and D. Porras, Symmetries and conservation laws in quantum trajectories: Dissipative freezing, Physical Review A **100**, 042113 (2019).
[39] R. Demkowicz-Dobrzański, M. Jarzyna, and J. Kołodyński, Quantum Limits in Optical Interferometry, Progress in Optics **60**, 345 (2015).
[40] A. I. Lvovsky, Squeezed Light, in *Photonics: Scientific Foundations, Technology and Applications*, Vol. 1 (John Wiley, Hoboken, NJ, USA, 2015) pp. 121–163.
[41] J. P. Dowling and K. P. Seshadreesan, Quantum optical technologies for metrology, sensing, and imaging, Journal of Lightwave Technology **33**, 2359 (2015).
[42] R. Schnabel, Squeezed states of light and their applications in laser interferometers, Physics Reports **684**, 1 (2017).
[43] K. Mølmer, Optical coherence: A convenient fiction, Physical Review A **55**, 3195 (1997).
[44] N. Bartolo, F. Minganti, J. Lolli, and C. Ciuti, Homodyne versus photon-counting quantum trajectories for dissipative Kerr resonators with two-photon driving, European Physical Journal: Special Topics **226**, 2705 (2017).
[45] R. J. Glauber, The quantum theory of optical coherence, Physical Review **130**, 2529 (1963).
[46] M. D. Cahalan, I. Parker, S. H. Wei, and M. J. Miller, Two-photon tissue imaging: Seeing the immune system in a fresh light, Nature Reviews Immunology **2**, 872 (2002).
[47] W. R. Zipfel, R. M. Williams, and W. W. Webb, Nonlinear magic: Multiphoton microscopy in the biosciences, Nature Biotechnology **21**, 1369 (2003).
[48] N. G. Horton, K. Wang, D. Kobat, C. G. Clark, F. W. Wise, C. B. Schaffer, and C. Xu, In vivo three-photon microscopy of subcortical structures within an intact mouse brain, Nature Photonics **7**, 205 (2013).
[49] M. A. Taylor and W. P. Bowen, Quantum metrology and its application in biology, Physics Reports **615**, 1 (2016).
[50] J. Gea-Banacloche, Two-photon absorption of nonclassical light, Physical Review Letters **62**, 1603 (1989).
[51] H.-B. Fei, B. Jost, S. Popescu, B. Saleh, and M. Teich, Entanglement-Induced Two-Photon Transparency, Physical Review Letters **78**, 1679 (1997).
[52] N. Georgiades, E. Polzik, K. Edamatsu, H. Kimble, and a. Parkins, Nonclassical Excitation for Atoms in a Squeezed Vacuum, Physical Review Letters **75**, 3426 (1995).
[53] L. Upton, M. Harpham, O. Suzer, M. Richter, S. Mukamel, and T. Goodson, Optically excited entangled states in organic molecules illuminate the dark, Journal of Physical Chemistry Letters **4**, 2046 (2013).
[54] J. P. Villabona-Monsalve, O. Calderón-Losada, M. Nuñez Portela, and A. Valencia, Entangled Two Photon Absorption Cross Section on the 808 nm Region for the Common Dyes Zinc Tetraphenylporphyrin and Rhodamine B, Journal of Physical Chemistry A **121**, 7869 (2017).
[55] T. Li, F. Li, C. Altuzarra, A. Classen, and G. S. Agarwal, Squeezed light induced two-photon absorption fluorescence of fluorescein biomarkers, Applied Physics Letters **116**, 254001 (2020).
[56] B. R. Mollow, Two-photon absorption and field correlation functions, Physical Review **175**, 1555 (1968).
[57] M. G. Paris, Quantum estimation for quantum technology, International Journal of Quantum Information **7**, 125 (2009).
[58] L. Pezzé and A. Smerzi, Mach-Zehnder Interferometry at the Heisenberg Limit with Coherent and Squeezed-Vacuum Light, Physical Review Letters **100**, 073601 (2008).
[59] S. A. Schäffer, M. Tang, M. R. Henriksen, A. A. Jørgensen, B. T. Christensen, and J. W. Thomsen, Lasing on a narrow transition in a cold thermal strontium ensemble, Physical Review A **101**, 13819 (2020).
[60] C. Hamsen, K. N. Tolazzi, T. Wilk, and G. Rempe, Two-Photon Blockade in an Atom-Driven Cavity QED System, Physical Review Letters **118**, 133604 (2017).
[61] T. Serikawa, J.-i. Yoshikawa, K. Makino, and A. Frusawa, Creation and measurement of broadband squeezed vacuum from a ring optical parametric oscillator, Optics Express **24**, 28383 (2016).
[62] S. Ast, M. Mehmet, and R. Schnabel, High-bandwidth squeezed light at 1550 nm from a compact monolithic PPKTP cavity, Optics Express **21**, 13572 (2013).
[63] G. Patera, N. Treps, C. Fabre, and G. J. De Valcárcel, Quantum theory of synchronously pumped type i optical parametric oscillators: Characterization of the squeezed supermodes, European Physical Journal D **56**, 123 (2010).

Figures

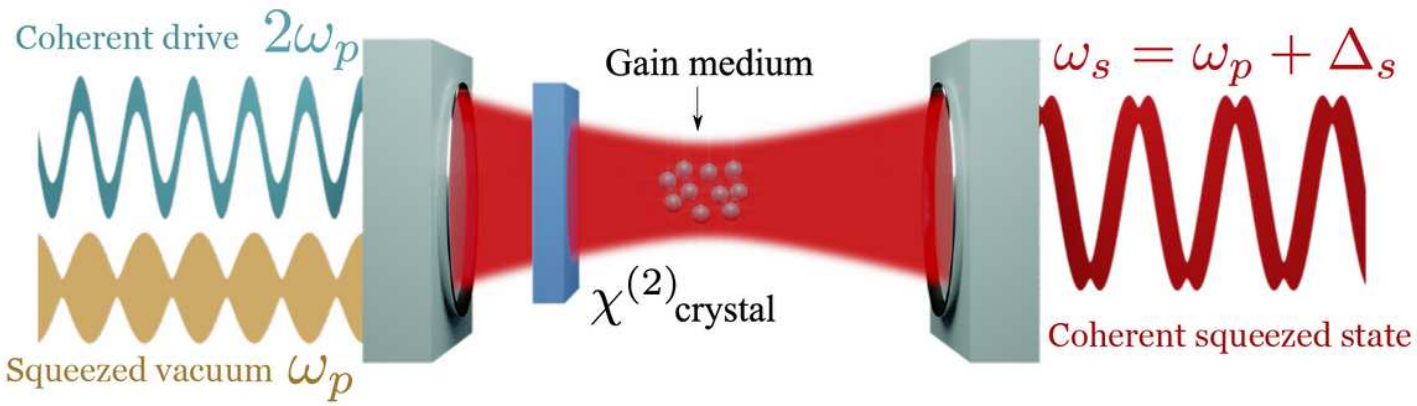

Figure 1

Sketch of the proposed setup: a single cavity mode of frequency ωc = ωp + Δc (with Δc << ωp) is parametrically driven through the down-conversion of pump photons of frequency 2ωp by a non-linear crystal χ(2). The cavity includes a gain medium (e.g. an ensemble of two-level atoms) and is driven by a broadband squeezed vacuum centred at the frequency ωp to stabilize lasing action. If the laser is imposed with a well-defined phase, the output emission corresponds to a coherent squeezed state of frequency ωs = ωp + Δs.

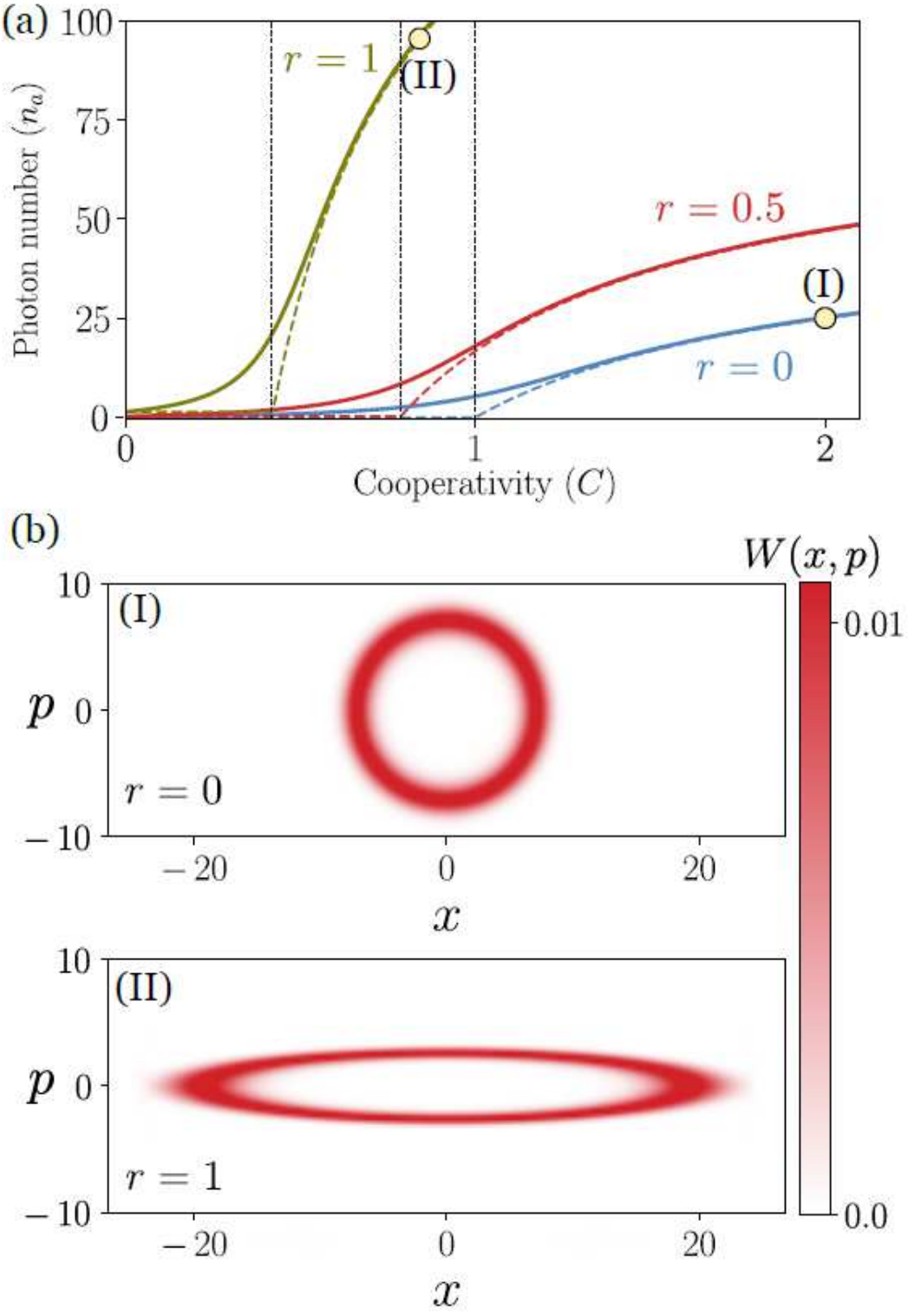

Figure 2

(a) Lasing phase transition in terms of photon number versus cooperativity, for different values of the squeezing parameter r. Saturation photon number set as nq = 50. Vertical lines mark the critical points, which are reduced for increasing r. Solid lines: exact numerical result. Dashed lines: mean field prediction. (b) Wigner function of the steady state corresponding to points (I) and (II) in panel (a), with r = 0 and 1 respectively, and θ = π.

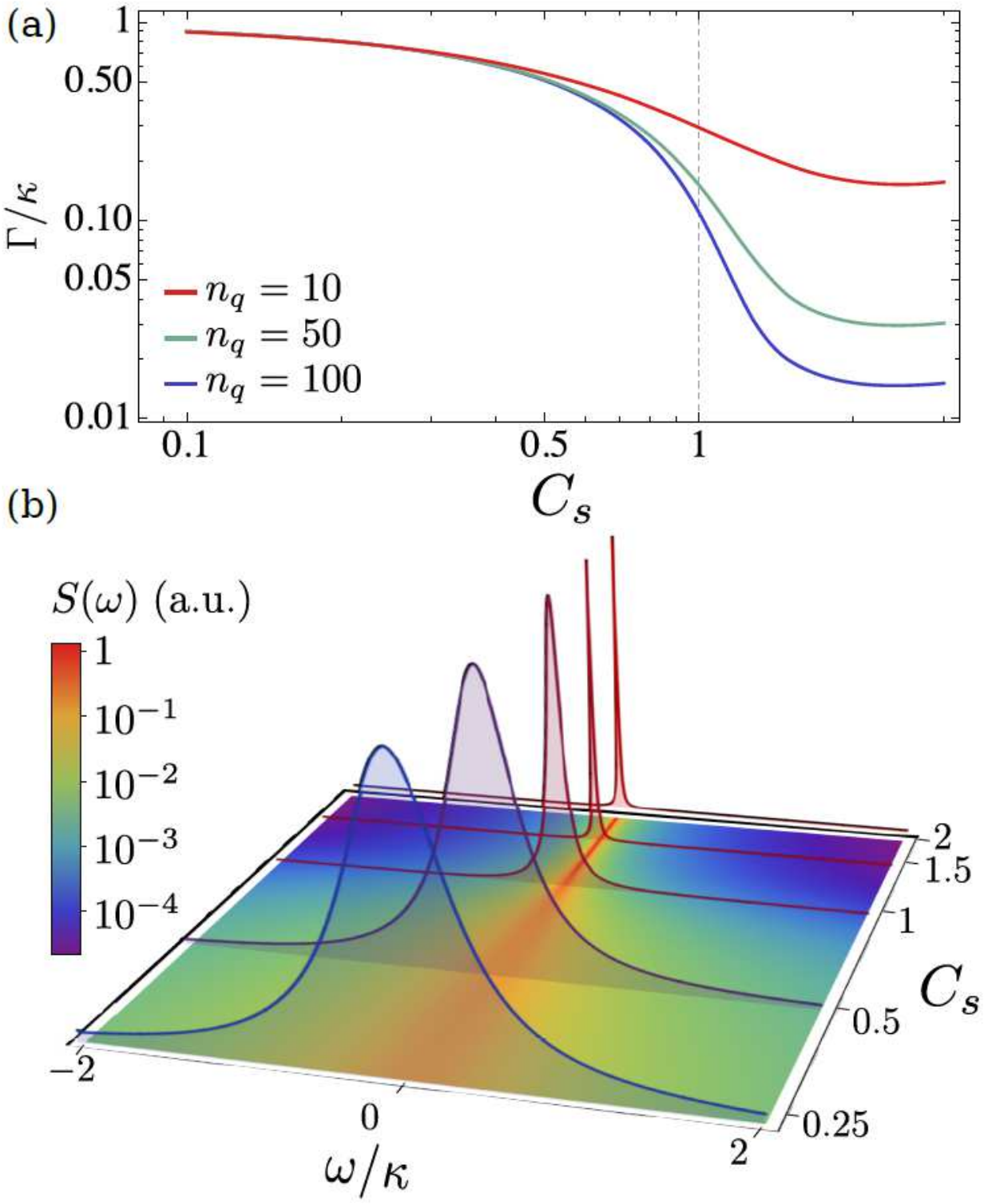

Figure 3

Line narrowing of the emission spectrum in a squeezed laser. (a) Emission linewidth (related to phase diffusion rate) versus cooperativity Cs for different values of saturation photon number nq. This result depends on r only through Cs. (b) Spectrum versus cooperativity Cs for saturation photon number nq = 100. Frequency defined with respect to the squeezed mode frequency ωs.

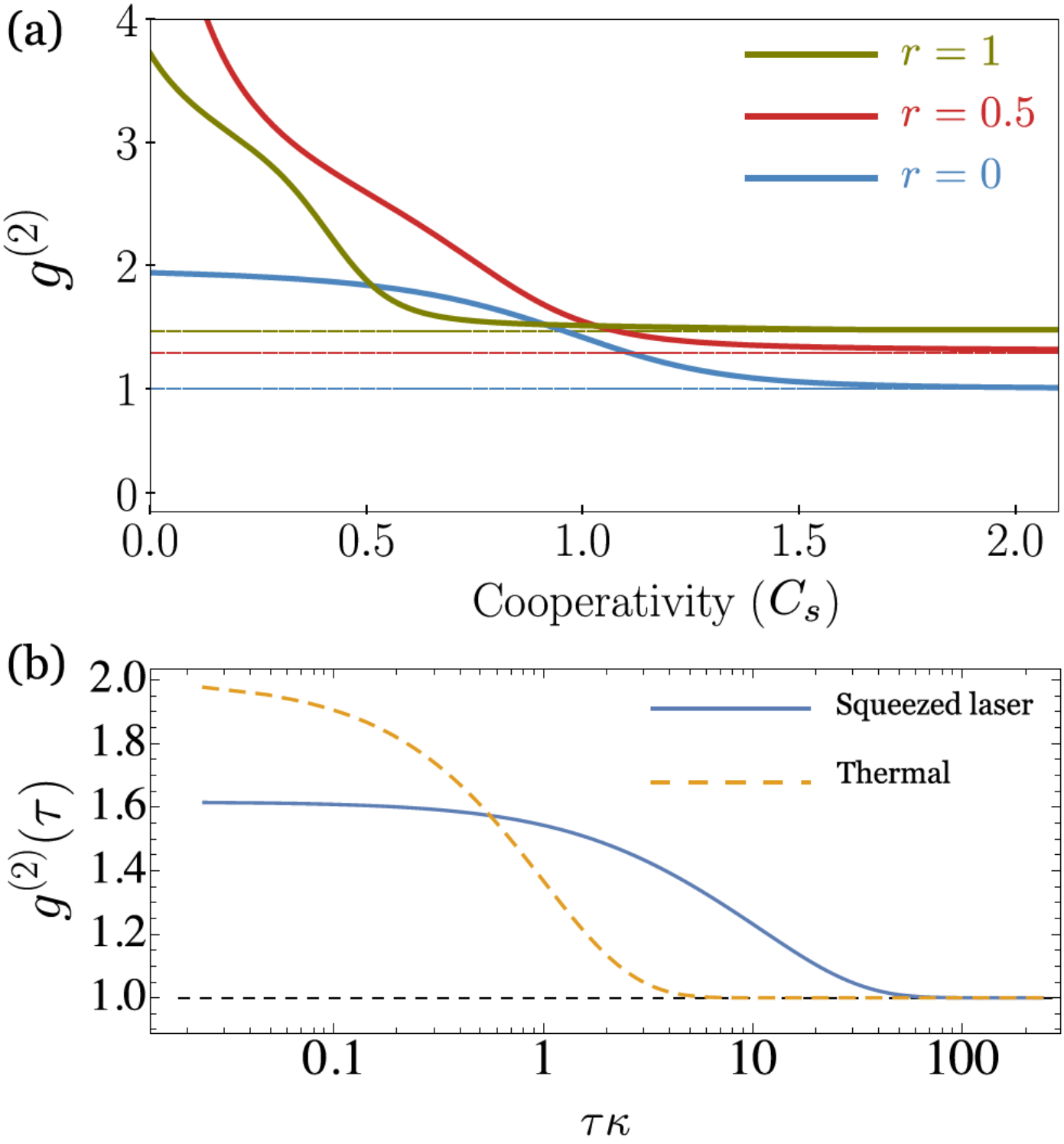

Figure 4

Second-order correlation function. (a) Zero-delay second-order correlation function versus Cs for three values of squeezing parameter r and nq = 50. Dashed lines correspond to the limit in the lasing regime given by Eq. (14). (b) g(2)(τ) of the squeezed laser displaying positive correlations surviving for extremely long correlation times ⍰ 1/Γ. A thermal state, showed for comparison, displays a much shorter positive correlation time of the order 1/κ. Parameters: Cs = 1.5, r = 1, nq = 50.

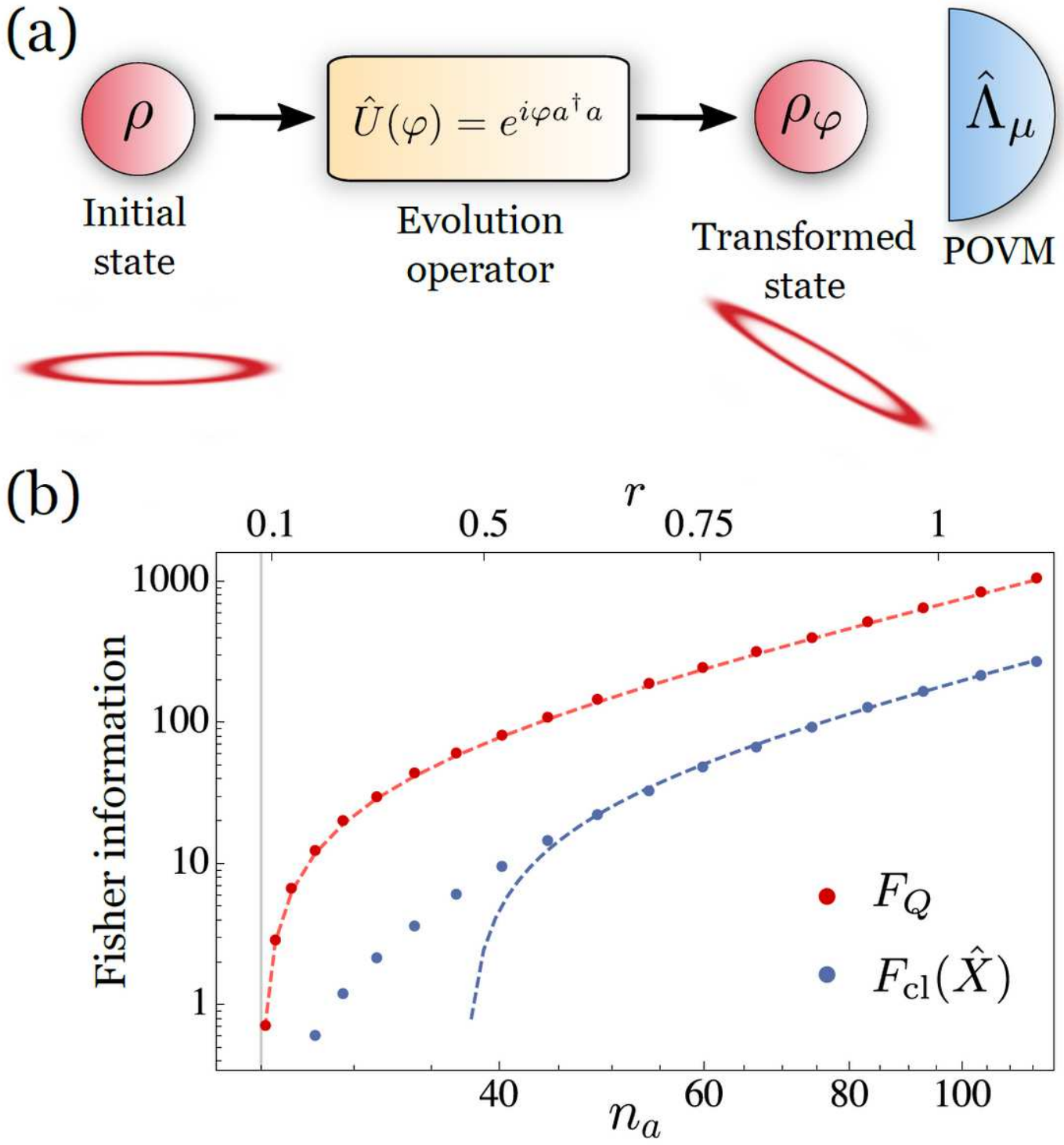

Figure 5

(a) Quantum parameter estimation. (b) Fisher information versus average photon number.